DIRECTED ENERGY DEPOSITION OF A CEMENTED TUNGSTEN CARBIDE ROTARY BURR PROTOTYPE

Emma Molobi
School of Chemical and Metallurgical Engineering & DSI-NRF Centre of Excellence in Strong Materials
University of the Witwatersrand
Johannesburg, South Africa
emma.molobi@transnet.net

Natasha Sacks
Department of Industrial Engineering & DSI-NRF Centre of Excellence in Strong Materials
Stellenbosch University
Stellenbosch, South Africa
natashasacks@sun.ac.za

Maritha Theron
National Laser Centre
Council for Scientific and Industrial Research
Pretoria, South Africa
mtheron@csir.co.za

***Abstract*—In this study a cemented tungsten carbide rotary burr prototype was fabricated using directed energy deposition based on an optimal parameter set which was previously derived from a full factorial design of experiments matrix approach. Finite element analysis under static conditions was carried out on the burr to understand the possible geometric stress raisers and stresses during assimilated operation. Initial field tests were done to assess the functional performance of the prototype, and comparisons were made against a conventionally manufactured burr.**

Keywords—directed energy deposition, cemented tungsten carbide, stress, rotary burr

I. INTRODUCTION

Directed energy deposition (DED) is an additive manufacturing (AM) process which directs energy from a laser or electron beam heat source into a narrow, focused region to melt the feedstock powder as it is deposited onto the substrate [1], [2]. Laser engineered net shaping (LENS®) is a DED process which has been successfully used in the fabrication of a range of materials such as stainless steels, nickel alloys, composites and graded materials [3]. The LENS® process fabricates components by interpreting the STL file format of a computer aided design (CAD) model of the part to be manufactured. The CAD model is divided into thin orthogonal layers in the z-axis and the data for each layer is interpreted and translated into laser scanning paths to fabricate a single layer [4]. The layers are fabricated by first generating an outline of each feature and then the nozzle moves up by a z-increment in order to deposit more layers until fabrication is complete. The advantages of DED processes in comparison with conventional manufacturing processes such as sintering and subtractive manufacturing includes the production of near net shaped components, rapid production, limited usage of fixtures and no requirement for patterns [5].

There have been studies into the application of the LENS® technology in the fabrication of cemented tungsten carbide (WC) alloys. Xiong et al. [6], [7], [8] investigated its applicability in the fabrication of cobalt (Co) cemented WC while Davoren et al. [9] investigated the deposition of a WC-Monel alloy.

Department of Science and Innovation and the National Research Foundation in South Africa.

The National Laser Centre (NLC) at the Council of Scientific and Industrial Research (CSIR).

LENS® has also been successfully used in the repair of titanium manufactured components [10] and the fabrication of Inconel free forms [2]. However, the commercialization aspect of the LENS® fabrication of cemented WC does not appear to have been achieved yet. This study investigated the fabrication of an iron-based cemented WC rotary burr prototype using the LENS® process.

II. EXPERIMENTAL METHODS

A. Laser deposition

In preparation for deposition the prototype rotary burr was designed to have a shank diameter of 6 mm, burr diameter and length of 12 x 25 mm, and a total length of 65 mm. It was designed without a rotary end cut and all designs were based on DIN 8033 and the PFERD burr catalogue [11]. CAD models were made using Creo Parametrics which uses history based parametric modelling which entails building a 3D geometry, piece by piece by using 2D sketches. Once the CAD model was established it was saved as an STL format and then sliced along the z-axis into layers which translated into laser scanning paths.

An Optomec 850-R LENS® machine with a 1kW IPG fiber was used to manufacture two WC-10wt% FeCr cylindrical rotary burr prototypes at atmospheric conditions using the parameters shown in TABLE I which were derived in an earlier study. For the manufacture of one of the burrs the substrate was pre-heated prior to deposition. The burrs were sectioned from the substrate using a Struers Secotom-10 precision cutting machine, with a 12 cm diameter Struers diamond coated wheel at a cutting speed of 3500 rpm and a feed rate of 0.015 mm/s. The dimensions of the rotary burrs were measured using a Vernier calliper and compared to the dimensions of a conventionally manufactured burr to verify part accuracy.

TABLE I. Near optimum parameters for LENS® deposition

Process parameter	**Value**
Laser power (W)	200
Traverse speed (mm/s)	3.2
Powder feed rate (g/min)	12.2
Z-increment (mm)	0.2
Stand-off distance (mm)	8
Laser spot size (mm)	1.4

B. *Finite Element Analysis (FEA) and Benchmarking Tests*

FEA analysis was done using MSC Patran® and Nastran® software at static conditions to verify the location of the largest von Mises stresses. A structural analysis using a first principle approach and a FEA linear static assessment were done. The performance matrix used for the analysis was a power tool with a rotational speed of 32000 rpm and a cutting speed of 600 m/min. Equations (1) to (4) show the calculations used for torque and maximum shear stress.

$$\tau_{max} = k_{ts}\,(Tr/J) \quad (1)$$

$$T = (P \times 30)/\pi\eta \quad (2)$$

$$J = \pi(2r)^4)/32 \quad (3)$$

$$r = d/2 \quad (4)$$

τ_{max} is the maximum shear stress (MPa), k_{ts} is the stress concentration factor which is 1 for brittle materials [12], T is the torque, P is the power of the rotary tool, η is the rotational speed (rpm), J is the polar second moment of area, r is the radius of the burr shank (m), and d the diameter of the shank. The finite element was meshed using a four node tetrahedral (TET4) element type mesh. The analysis boundary conditions was a fixed end at the burr shank. The properties of the burr used for the analysis was an elastic modulus (E) of 513 MPa [13], and a Poisson ratio (υ) of 0.3 [14].

The rotary burr which was deposited on a preheated substrate fractured during removal from the substrate. Hence the prototype burr without substrate preheat was benchmarked against conventionally manufactured burrs in terms of removal of previously deposited weld material. A weld deposit made from AWS A5.1 E7018-1 having a tensile strength of 490 – 550 MPa [15] was used for the test. The weld deposit was machined at one-minute intervals for a total time of five minutes using a handheld rotary tool with a cutting speed of 600m/min and rotational speed of 32000 rpm. The thickness of the weld deposit and substrate was measured using the Vernier calliper after each interval to record the amount of material removed by the burr. The burr which removed more material in the allocated time was selected as the better performing burr.

III. RESULTS AND DISCUSSION

A. *CAD model and FEA analysis*

Fig. 1 shows the CAD model of the rotary burr prototype.

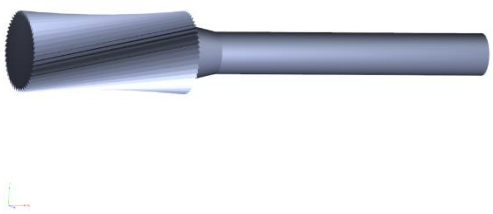

Fig. 1. Side view of rotary burr

Fig. 2 shows the FEA model and the load/boundary conditions of the cylindrical rotary burr. The maximum shear stresses acting on the rotary burr prototype was calculated to be 6.84 MPa and the torque to be 0.29 Nm.

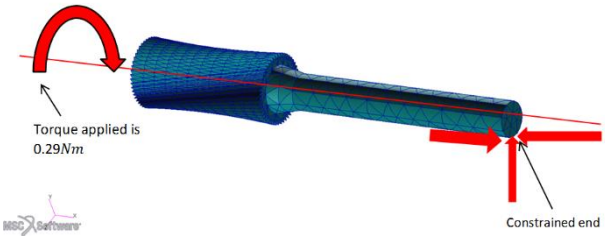

Fig. 2. Applied operational loads and boundary conditions

FEA showed that the fillet junction area which connects the shank and the burr head acts as a stress raiser and experienced the highest stress concentration (Fig. 3). Internal stresses will exist in sharp corners and fillet radii because of the abrupt change in shape. In order to mitigate this a large fillet radius should be incorporated in the 3D CAD model so that there is enough space for the distribution of the internal stresses. This analysis showed that if failure should occur, the area with the highest stress concentration would be the first to fail.

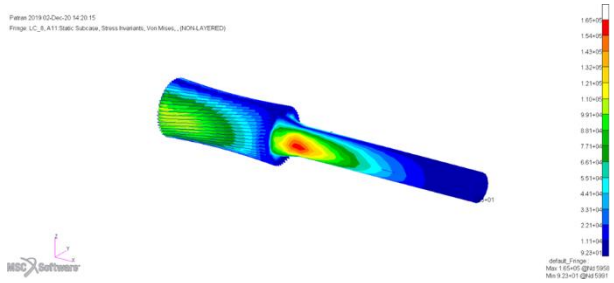

Fig. 3. Von Mises stress due to imposed load

B. *Fabrication of the Prototype Burr*

The rotary burr prototype was manufactured in a three-step process (Fig. 4) without the use of fixtures, compared to the nine-step conventional process (Fig. 5), which shows the benefits of using AM. The LENS® fabrication time per burr was 04h04min30sec in comparison to the conventional sintering cycles of 15-20 hours. The flutes on the burr were partially visible in comparison to the conventionally manufactured rotary burrs and this was due to the rougher surface finish imparted by the DED process. The powder utilization of this process was calculated to be 50.2% by weighing the initial amount of powder used for the deposition process and the amount of powder which was not deposited into the molten pool. The low powder efficiency of the LENS® process shows that feasibility of the process will depend on the ability to recycle the powder.

Fig. 4. LENS® process flow for the manufacture of the prototype burr

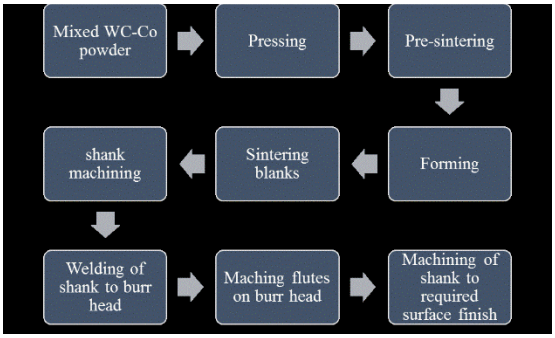

Fig. 5. Process flow in the conventional manufacturing of hard metal burrs [16].

Fig. 6 shows the rotary burr during deposition and Fig. 7 shows the final burr.

Fig. 6. LENS fabrication of the cylindrical rotary burr

Fig. 7. LENS® fabrication of a cylindrical rotary burr with preheat of 250°C

The part accuracy was not compliant with the 3D CAD model input dimensions (Table II), showing that the prototype requires final machining in order to achieve accurate dimensions, visible flutes and an acceptable surface finish. In addition the burr visually showed distortion in the form of a concave shape, this shape was in accordance to the CAD model which also showed a concave burr. Final machining will increase the number of production steps required before the burr can be deemed market-ready, however, the LENS® processes will then require 4 manufacturing steps which is still less than the than the conventional process.

Table II. Dimensions of the LENS® fabricated and sintered WC burrs

Burr dimensions	**Shank diameter (mm)**	**Burr diameter (mm)**	**Burr length (mm)**
CAD model	6	12	25+5(to accommodate removal from substrate)
LENS® deposited WC-10wt% FeCr	7.26	11.74	26.51
Sintered WC-Co	6.04	11.99	25.04

C. Field Testing of the Rotary Burr Prototype

The performance of the prototype burr was based on the removal of previously deposited welds. This was compared with conventionally manufactured cemented WC burrs. Fig. 8 shows the built-up weld requiring machining and Fig. 9 shows the performance of the prototype burr in comparison to the sintered burr in machining the weld surface. The prototype burr failed at the fillet junction as predicted by FEA after machining 0.22 mm of the weld in 2 minutes. The sintered burr did not fail and testing was stopped after 5 minutes.

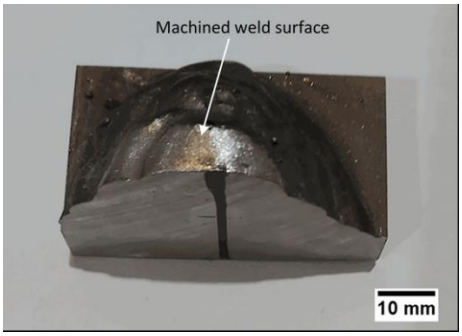

Fig. 8. Machined weld surface

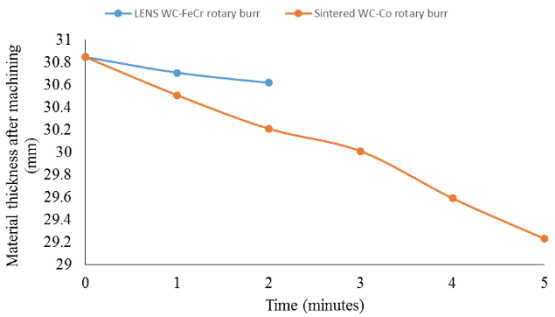

Fig. 9. Machining performance of LENS® fabricated and sintered cylindrical rotary burrs

During machining of the weld it was observed that the prototype burr vibrated extensively, which is believed to have contributed to failure of the burr. Fig. 10 shows the failed burr indicating a three-point brittle fracture with no evidence of plastic deformation. This indicates that only low fracture energy was required for the failure to occur.

Fig. 10. Fracture surface of LENS® fabricated rotary burr

IV. CONCLUSION

A WC-10wt% FeCr prototype cylindrical rotary burr was fabricated using the LENS® technology. FEA analyses predicted that the fillet junction area which connects the shank and the burr head would be a point of weakness as a stress raiser and would experience the highest stress concentration. This prediction was shown to be accurate when the burr failed at this junction area during machining tests. The conventionally manufactured cemented tungsten carbide cylindrical rotary burr outperformed the prototype. However, the prototype showed potential as it failed at the shank and not the burr head. One of the limitations of the prototype was the rough surface finish due to the DED process which possibly enhanced the vibrations experienced during machining of the weld thereby leading early failure. In addition to the rough surface finish the dimensional accuracy of the burr did not comply to the CAD model, hence final machining will be required in order to explore the feasibility of LENS® deposited cemented WC burrs.

ACKNOWLEDGEMENT

The authors wish to acknowledge the financial support received from the Department of Science and Innovation and the National Research Foundation in South Africa (Grant Nos: 41292 and 129313). The National Laser Centre (NLC) at the Council for Scientific and Industrial Research (CSIR) is acknowledged for use of the LENS® machine as well as technical support (Grant No: LREPA25). Opinions expressed and conclusions arrived at are those of the authors and are not necessarily to be attributed to the funders.

REFERENCES

[1] I. Gibson, D. .Rosen, and B. Stucker, *Additive ManufacturingTechnologies: Rapid Prototyping to Direct Digital Manufacturing*. Springer, 2014.

[2] J. Zhang and Y. Jung, *Additive Manufacturing Materials, Processes, Quantification and Applications*. Butterworth-Heinemann, 2018.

[3] M. Griffith, L. Harwell, T. Romero, E. Schlienger, C. Atwood, and J. Smugeresky, "Multi-Material Processing by LENS," in *The Solid Freeform Fabrication Symposium*, 1997, pp. 11–13.

[4] C. Atwood *et al.*, "Laser engineered net shaping (LENS™): A tool for direct fabrication of metal parts," pp. E1–E7, 2018, doi: 10.2351/1.5059147.

[5] T. .Sudarshan and T. .Srivatsan, *Additive Manufacturing, Innovations, Advances, and Applications*, 1st ed. New York: Taylor & Francis Group, 2015.

[6] Y. Xiong, J. E. Smugeresky, L. Ajdelsztajn, and J. M. Schoenung, "Fabrication of WC-Co cermets by laser engineered net shaping," *Mater. Sci. Eng. A*, vol. 493, no. 1–2, pp. 261–266, 2008, doi: 10.1016/j.msea.2007.05.125.

[7] Y. Xiong, J. E. Smugeresky, E. J. Lavernia, and J. M. Schoenung, "Processing and microstructure of WC-CO cermets by laser engineered net shaping," *19th Annu. Int. Solid Free. Fabr. Symp. SFF 2008*, pp. 116–127, 2008.

[8] Y. Xiong, J. E. Smugeresky, and J. M. Schoenung, "The influence of working distance on laser deposited WC-Co," *J. Mater. Process. Technol.*, vol. 209, no. 10, pp. 4935–4941, 2009, doi: 10.1016/j.jmatprotec.2009.01.016.

[9] B. Davoren, N. Sacks, and M. Theron, "Laser engineered net shaping of WC-9.2wt%Ni alloys: A feasibility study," *Int. J. Refract. Met. Hard Mater.*, vol. 86, no. June 2019, p. 105136, 2020, doi: 10.1016/j.ijrmhm.2019.105136.

[10] J. Ruan, T. .Sparks, Z. Fan, and J. .Stroble, "A Review of Layer Based Manufacturing Processes for Metals," Rolla, 2006.

[11] "Pferd Catalogue," *Pferd*. https://www.pferd.com/images/WZH_22_202_en_72_dpi.pdf. [Accessed 28 October 2020] (accessed Apr. 01, 2014).

[12] R. Budynas and J. .Nisbett, *Shingley's Mechanical Engineering Design*, 10th ed. New York: McGraw-Hill Education, 2015.

[13] C. M. Fernandes *et al.*, "Mechanical characterization of WC-10wt% AISI 304 cemented carbides," *Mater. Sci. Eng. A*, vol. 618, pp. 629–636, 2014, doi: 10.1016/j.msea.2014.09.064.

[14] K. Liu, "Tungsten Carbide," Croatia, 2012.

[15] A. W. Society, "AWS A5.1/5.1M: Specification for Carbon Steel Electrodes for Shielded Metal arcWelding," Florida, 2012.

[16] "Liyotools." http://liyotools.com/production-process-carbide-burrs/ (accessed Oct. 14, 2020).